SUPPLEMENTAL MATERIAL

CEMENTED LAYERS AND GRAIN-DENSITY INTERPOLATION

The section from 130 to 136 mbsf in the AND1-B core is presented as an example how carbonate cement concentrated in thin micritic beds is expressed in the physical properties (Fig. S 1). The cemented intervals are visible in core images by their brighter color. Four cemented intervals (1 to 4 in Fig. S 1) can be identified in the example, of which only 1 is a distinct micritic layer, wheras 2 and 3 are more nodular and 4 is nodular to layered. Carbonate cement leads to a strong increase in velocity, significant to weak increase and decrease in WBD and FP, respectively. Electrical conduction, expressed as sensor response (Niessen et al., 2007), is decreased except for intervals with nodular cement (Fig. S 1). A strong effect of cement on porosity (almost complete reduction of voids) is only notable in the micritic layer at 132.3 mbsf. Such layers are quantitatively rare in the entire core although a detailed analysis of cemented layers of AND-1B in terms of physical properties has not yet been carried out.

The section from 130 to 136 mbsf can also be used to demonstrate the result of the grain-density interpolation (Fig. S 1). Since the lithology varies on a higher level of resolution than data points of grain densities from discrete samples are available (approximately one per meter core, Fig. S1), not all changes in lithology are covered by data points based on measured grain density. The approach of grain-density interpolation (Fig. S1), as described under METHODS of the paper, simulates differences in grain densities in different lithologies very well. This does not include cemented layers because so far no numerical record of cement as part of the lithology is available for the AND-1B core. As cemented layers are not well represented by grain-density samples the exact porosities of these layers remain undetermined.

ALGORITHMS USED TO EXPRESS AND CALCULATE NORMAL CONSOLIDATION FOR VOID RATIOS AS A FUNCTION OF EFFECTIVE STRESS

The trends of normal consolidation for different lithologies as presented in Figure 9 (functions A to E) are calculated as described below.

Effective Stress

For functions A (diatom ooze), C (pelagic clay) and D (terrigenous sediments), WBD were calculated using regression equations given in Hamilton (1976) valid to depths (d) of 500 mbsf, 300 mbsf and 1000 mbsf, respectively.

A: $WBD = 1.240 + 0.757\ (d) - 0.685\ (d^2)$;

C: $WBD = 1.357 + 1.338\ (d) - 0.248\ (d^2)$;

D: $WBD = 1.53 + 1.395\ (d) - 0.617\ (d^2)$.

Effective stress was then calculated after equation (4) to (6) with ρ_i as WBD above and ρ_w as assumed constant with 1.03 gcm^{-3}.

For function B (diatom ooze) effective stress is given by Bryant and Rack (1990) for 13 data points to 3,000 kPa. The linear trend from 400 kPa to 3,000 kPa was extrapolated to 4,500 kPa.

Void Ratios

For functions A (diatom ooze), C (pelagic clay) and D (terrigenous sediments), FP were calculated using regression equations given in Hamilton (1976) valid to depths (d) of 500 mbsf, 300 mbsf and 1,000 mbsf, respectively.

A: $FP = 0.861 - 0.549\ (d) + 0.492\ (d^2)$;

C: $WBD = 0.814 - 0.813\ (d) - 0.164\ (d^2)$;

D: $WBD = 0.72 - 0.8165\ (d) + 0.361\ (d^2)$.

Void ratios were then calculated after equation (3). For function B (diatom ooze) void ratios are given by Bryant and Rack (1990) for 13 data points to 1.8. The linear trend from 3.5 to 1.8 was extrapolated to 1.22. For function E (diamicton) it is assumed that that initial void ratio of 1 at a stress

level of 10 kPa is reduced to void ratio of 0.4 at an effective stress of 10^5 kPa.

Hypothetical Void Ratios of AND-1B for normal consolidation

For the plots of void ratios versus effective stress of different lithologies (B, C, D, E) regressions were determined using Kaleidagraph™ (Synergy Software). The regression for trend A was not used because trends A and B are nearly similar below a stress level of 200 kPa where most of the AND-1B data were determined. For functions B, C and D best fits were achieved by 5th order polynomials with the general term:

$VR = t + u* ES + w*ES^2 + x*ES^3 + y*ES^4 + z*ES^5$,

with VR = Void Ratio and ES = Effective Stress. The constants t, u,w,x,y and z as well as the correlation coefficients R for functions B, C, and D are summarized in Table S1. For the assumed normal consolidation of diamictites (E) the regression is a log function:

$VR = 1.1951 - 0.2 \log (ES)$, with R=0.99992

From the effective stress of AND-1B sediments hypothetical void ratios were calculated according to different lithology. Regression B was used for diatomites. Regression C was used for mudstones to a depth of 200 mbsf (equivalent to 1,664 kPa). Below 200 mbsf regression D was used to calculate hypothetical void ratios of mud stones because both regressions merge at about 1,650 kPa. Hypothetical void ratios of other lithologies (mostly sandstones) and diamictites were calculated using regressions D and E, respectively. The advantage of this approach is that hypothetical void ratios are calculated for different stress levels and not as a function of depth below sea floor. This accounts for the individual field consolidation of the different lithologies at the AND-1B site. Thus the hypothetical and measured AND-1B void ratios are better comparable to other sites around Antarctica, where the lithologies are more uniform and the field consolidation is different from that of AND-1B.

COMPARISON OF AND-1B DIATOMITE FRACTIONAL POROSITIES WITH DATA FROM DIATOMACEOUS INTERVALS IN OTHER MARINE SEDIMENT CORES (REFERENCE DATA)

Fractional porosity records of sediment cores from various drill sites around Antarctica and in the Southern Ocean, including the second ANDRILL core AND-2A, were compiled to serve as reference data sets for assessing porosity features of the AND-1B diatomites (Fig. S2, Table S2). These collected data provide a good coverage of depositional features in terms of distance from the Antarctic continent and therefore degree of influence of the ice sheet as well as in terms of geologic time intervals ranging from the Holocene back to the Upper Cretaceous. The reference data from the Southern Ocean are complemented by reference curves for different types of deep-sea sediments as presented by Hamilton (1976). The reference curve for diatom ooze is a composite curve of cores from the DSDP sites 19-188 and 19-192 in the Bering Sea. Screen descriptions of smear slides indicate siliceous contents of 65-95 % (screen descriptions from http://www.ngdc.noaa.gov/mgg/geology/dsdp/data/). AND-1B diatomite intervals are characterized by a signature of systematically lower fractional porosities compared to the majority of the reference data (Fig. S2). This is partly compromised by a large scatter in the reference porosities in the upper 150 m, where values are observed that are even lower than that of the Hamilton reference curve for terrigenous sediment and pelagic clay. The scatter is related to the broad coverage of subtle variations within the overall lithologic composition of "diatomaceous sediments" ranging from "diatom ooze" to "muddy diatom ooze" and "terrigenous detritus rich diatom ooze" (Tab. S2). However, from about 200 mbsf most of the reference data follow the Hamilton reference curve for deep-sea diatomaceous ooze quite closely, whereas AND-1B porosities are offset from the reference curve towards lower values by about 0.1. AND-1B diatomite intervals are thus relatively over-compacted compared to the majority of the reference data. As described in the discussion of the paper vertical loading of ice sheets during glacial periods account for most of the porosity differences between the AND-1B diatomites and the reference data. Some differences however are also the result of different conditions of field consolidation in the reference data. At the same depth interval a sequence consisting entirely of diatomaceous ooze is less consolidated as diatomites of AND-1B, which are intercalated with and overlain by heavier diamictites. In this sense, and as expressed in the paper, the AND-1B core is unique and can only be compared with reference data from other cores if the porosity is expressed as a function of effective stress.

REFERENCES CITED

Barker, P.F., Camerlenghi, A., Acton, G.D., et al., eds., 1999, Proceedings of the Ocean Drilling Program, Initial Reports, v. 178, College Station, TX (Ocean Drilling Program).

Barker, P.E, Kennett, J.P., et al., eds., 1988, Proceedings of the Ocean Drilling Program, Initial Reports, v. 113: College Station, TX (Ocean Drilling Program), p 5–11. doi:10.2973/odp.proc.ir.113.102.

Barron, J., Larsen, B., et al., eds., 1989, Proceedings of the Ocean Drilling Program, Initial Reports , v. 119, College Station, TX (Ocean Drilling Program).

Barrett, P.J., Carter, L., Dunbar, G.B., Dunker, E., Giorgetti, G., Harper, M.A., McKay, R.M., Niessen, F., Nixdorf, U., Pyne, A.R., Riesselmann, C., Robinson, N., Hollis , C., and Strong, P., 2005, Oceanography and sedimentation beneath the McMurdo Ice Shelf in Windless Bight, Antarctica: Antarctic Data Series 25, Research Centre, Victoria University of Wellington, 100 p.

Bryant, W.R., and Rack, F.R., 1990, Consolidation characteristics of Weddell Sea sediments: results of ODP Leg 113, *in* Barker, P.F., Kennett, J.P., et al., eds.: Proceedings of the Ocean Drilling Program Scientific Results, v. 113, College Station, TX (Ocean Drilling Program), p. 211–223.

Hamilton, E.L., 1976, Variations of density and porosity with depth in deep-sea sediments: Journal of Sedimentary Petrology, v. 46, p. 280-300.

Niessen, F., Magens, D., Gebhardt, A.C. and the ANDRILL-MIS Science Team, 2007, Physical Properties of the AND-1B Core, ANDRILL McMurdo Ice Shelf Project, Antarctica: Terra Antartica, v. 14, no. 3, p. 155-166.

Schlich, R., Wise, S.W., Jr., et al., eds., 1989, Proceedings of the Ocean Drilling Program, Initial Reports, v. 120, College Station, TX (Ocean Drilling Program).

Figure captions

Figure S1. AND-1B detailed physical properties log 130 to 136 mbsf. Vp and Resistivity (electrical conduction, sensor response) from Niessen et al. (2007). Lithology after Krissek et al. (2007). Core images from weblink *coreref.org/projects/and1-1b/viewer/130*. Density (WBD), grain density (GD) and fractional prosity (FP) this study. Dots in the plot of grain density are data from discrete samples. The line interpolates GD to the same vertical resolution as physical properties are measured on whole core (dots in the other plots) as described in text. For data in red boxes core images

are shown. Layers with carbonate cement are highlighted in yellow and labeled 1 to 4.

Figure S2. AND-1B fractional porosities of DU-II to DU-XIII (see Fig. 6 for details) in comparison with reference porosity data from diatomaceous intervals in DSDP and ODP sediment cores from the Southern Ocean (for detailed information on reference data see Table S2, for locations see Figure 1). Reference porosities were calculated from GRAPE measurements using equation (2). Reference curves for diatomaceous ooze, pelagic clay and terrigenous sediment from Hamilton (1976).

TABLE S1. CONSTANTS OF REGRESSION B, C, D SHOWN IN FIGURE 8

R = CORRELATION COEFFICIENT

	Regression		
Constant	B	C	D
t	5.17	4.3445	2.3798
u	-0.0038175	-0.0065453	-0.0011579
w	2.2374e-06	8.3914e-06	3.1612e-07
x	-6.9572e-10	-7.243e-09	-4.4536e-11
y	9.822e-14	3.4339e-12	3.03e-15
z	-4.7642e-18	-6.643e-16	7.8387e-20
R	0.99914	1	0.99896

TABLE S2. REFERENCE POROSITY DATA, SORTED BY RELATIVE DISTANCE TO THE ANTARCTIC CONTINENT

Drilling program / project	Leg + Site / core number	Latitude (°)	Longitude (°)	Water depth (m)	Age range	Lithology name from core description	Relative distance to Antarctic continent*	Porosity data reference source	Reference core description
DSDP	28-272	-77.13	-176.76	619	Upper Miocene - Mid-Miocene	terrigenous detritus rich (muddy) diatom ooze/diatomite	proximal: shelf	ODP data archive***	http://www.ngdc.noaa.gov/mgg/geology/dsdp/data/28/272/screen.txt
ODP	178-1098C	-64.86	-64.21	1010	Holocene	laminated/massive muddy/mud-bearing diatom ooze	proximal: inner shelf	IODP data archive****	Barker et al. (1999)
ODP	178-1099A	-64.95	-64.32	1400	Holocene	laminated/massive (muddy/mud-bearing) diatom ooze	proximal: inner shelf	IODP data archive	Barker et al. (1999)
ODP	178-1099B	-64.95	-64.32	1400	Holocene	laminated/massive (muddy/mud-bearing) diatom ooze	proximal: inner shelf	IODP data archive	Barker et al. (1999)

ODP	119-740A	-68.76	76.68	807	Quaternary - Upper Pliocene	diatom ooze	proximal: inner shelf	IODP data archive	Barron et al. (1989)
DSDP	28-268	-63.95	105.16	3529	Upper Pleistocene - Miocene	(clay mineral rich) diatom ooze	medial: continental rise	ODP data archive	http://www.ngdc.noaa.gov/mgg/geology/dsdp/data/28/268/screen.txt
ODP	178-1095B	-66.99	-78.49	3842	Late Pliocene - Mid-Miocene	(muddy) diatom ooze, muddy siliceous ooze	medial: continental rise	IODP data archive	Barker et al. (1999)
ODP	178-1096C	-67.57	-76.96	3153	Early Pliocene	muddy diatom ooze	medial: continental rise	IODP data archive	Barker et al. (1999)
DSDP	28-274	-69.00	173.43	3305	Quaternary - Lower Oligocene	terrigenous detritus rich (muddy) diatom ooze	medial: continental rise	ODP data archive	http://www.ngdc.noaa.gov/mgg/geology/dsdp/data/28/274/screen.txt

* open ocean not defined with respect to actual water depth but distance to Antarctic Shelf

** Southern McMurdo Sound Project

*** http://www.ngdc.noaa.gov/mgg/geology/dsdp/data
**** http://iodp.tamu.edu/janusweb/physprops/
For locations (Drilling program and Leg) see Figure 1.

TABLE S2. REFERENCE POROSITY DATA, SORTED BY RELATIVE DISTANCE TO THE ANTARCTIC CONTINENT (continued)

Drilling program / project	Leg + Site / core number	Latitude (°)	Longitude (°)	Water depth (m)	Age range	Lithology name from core description	Relative distance to Antarctic continent*	Porosity data reference source	Reference core description
ODP	113-689B	-64.52	3.10	2080	Quaternary/Lower Pliocene - Mid-Miocene	diatom ooze	distal: open ocean	IODP data archive	Barker et al. (1988)
ODP	113-690B	-65.16	1.20	2914	Quaternary/Upper Pliocene - Mid-Miocene	diatom ooze	distal: open ocean	IODP data archive	Barker et al. (1988)
ODP	113-696B	-61.85	-42.93	650	Upper Miocene - Mid-Miocene	(silty mud-bearing) diatom ooze, (mud-bearing) diatomite	distal: open ocean	IODP data archive	Barker et al. (1988)
ODP	119-736A	-49.40	71.66	629	Quaternary - Upper Pliocene	diatom ooze (with volcanic detritus)	distal: open ocean	IODP data archive	Barron et al. (1989)

ODP	119-736B	-49.40	71.66	628	Quaternary	diatom ooze (with volcanic detritus)	distal: open ocean	IODP data archive	Barron et al. (1989)
ODP	119-736C	-49.40	71.66	629	Upper Pliocene	diatom ooze	distal: open ocean	IODP data archive	Barron et al. (1989)
ODP	119-737A	-50.23	73.03	564	Lower Pliocene - Upper Miocene	diatom ooze	distal: open ocean	IODP data archive	Barron et al. (1989)
ODP	119-744C	-61.58	80.60	2308	Quaternary - Lower Pliocene	(calcerous) diatom ooze	distal: open ocean	IODP data archive	Barron et al. (1989)
ODP	119-745B	-59.60	85.85	4083	Quaternary - Lower Pliocene	(clay) diatom ooze, silty diatomaceous ooze	distal: open ocean	IODP data archive	Barron et al. (1989)
ODP	120-751A	-57.73	79.81	1634	Lower Pleistocene - Lower Pliocene	diatom ooze	distal: open ocean	IODP data archive	Schlich et al. (1989)
DSDP	28-265	-53.54	109.95	3581	Pleistocene - Lower Pliocene	(carbonate/nannofossil/ foraminifera rich) diatom ooze	distal: open ocean	ODP data archive	http://www.ngdc.noaa.gov/mgg/geology/dsdp/data/28/265/screen.txt
DSDP	28-266	-56.40	110.11	4167	Upper Pleistocene - Lower Miocene	(clay mineral rich) diatom ooze	distal: open ocean	ODP data archive	http://www.ngdc.noaa.gov/mgg/geology/dsdp/data/28/266/screen.txt

TABLE S2. REFERENCE POROSITY DATA, SORTED BY RELATIVE DISTANCE TO THE ANTARCTIC CONTINENT (continued)

Drilling program / project	Leg + Site / core number	Latitude (°)	Longitude (°)	Water depth (m)	Age range	Lithology name from core description	Relative distance to Antarctic continent*	Porosity data reference source	Reference core description
DSDP	29-278	-56.56	160.07	3675	Upper Pleistocene - Lower Miocene	diatom ooze, siliceous ooze	distal: open ocean	ODP data archive	http://www.ngdc.noaa.gov/mgg/geology/dsdp/data/29/278/screen.txt
DSDP	35-323	-63.68	-97.99	5004	Upper Pliocene - Lower Pliocene	clay mineral rich radiolaria rich muddy diatom ooze	distal: open ocean	ODP data archive	http://www.ngdc.noaa.gov/mgg/geology/dsdp/data/35/323/screen.txt
DSDP	36-328	-49.81	-36.66	5095	Pleistocene - Upper Eocene	diatom ooze	distal: open ocean	ODP data archive	http://www.ngdc.noaa.gov/mgg/geology/dsdp/data/36/328/screen.txt

DSDP	36-328B	-49.81	-36.66	5095	Pliocene - Lower Oligocene	(clay mineral rich) diatom mud	distal: open ocean	ODP data archive	http://www.ngdc.noaa.gov/mgg/geology/dsdp/data/36/328B/screen.txt
DSDP	36-329	-50.66	-46.10	1519	Pleistocene - Upper Miocene	(carbonate/clay mineral rich) diatom ooze, siliceous ooze	distal: open ocean	ODP data archive	http://www.ngdc.noaa.gov/mgg/geology/dsdp/data/36/329/screen.txt
DSDP	71-511	-51.00	-46.97	2589	Quaternary - Upper Eocene	(carbonate/nannofossil/ clay mineral rich) diatom ooze, siliceous ooze	distal: open ocean	ODP data archive	http://www.ngdc.noaa.gov/mgg/geology/dsdp/data/71/511/screen.txt
DSDP	71-512	-49.87	-40.85	1846	Pliocene - Mid-Miocene	(clay mineral rich) diatom mud/ooze	distal: open ocean	ODP data archive	http://www.ngdc.noaa.gov/mgg/geology/dsdp/data/71/512/screen.txt
DSDP	71-513	-47.58	-24.64	4373	Pleistocene - Lower Pliocene	clay mineral rich (muddy) diatom ooze	distal: open ocean	ODP data archive	http://www.ngdc.noaa.gov/mgg/geology/dsdp/data/71/513/screen.txt
DSDP	71-513A	-47.58	-24.64	4373	Lower Pliocene - Upper Oligocene	clay mineral rich (muddy) diatom ooze, clay mineral rich diatom mud	distal: open ocean	ODP data archive	http://www.ngdc.noaa.gov/mgg/geology/dsdp/data/71/513A/screen.txt
DSDP	71-514	-46.05	-26.86	4318	Quaternary - Lower Pliocene	clay mineral rich (muddy) diatom ooze, clay mineral rich diatom mud	distal: open ocean	ODP data archive	http://www.ngdc.noaa.gov/mgg/geology/dsdp/data/71/514/screen.txt
DSDP	19-188	53.75	178.66	2649	Upper Pleistocene - Upper Miocene	diatomaceous ooze	distal: slope	Hamilton (1976)	Hamilton (1976)
DSDP	19-192	53.01	164.71	3014	Upper Miocene - Mid-Miocene	diatomaceous ooze	distal: open ocean	Hamilton (1976)	Hamilton (1976)

131

132

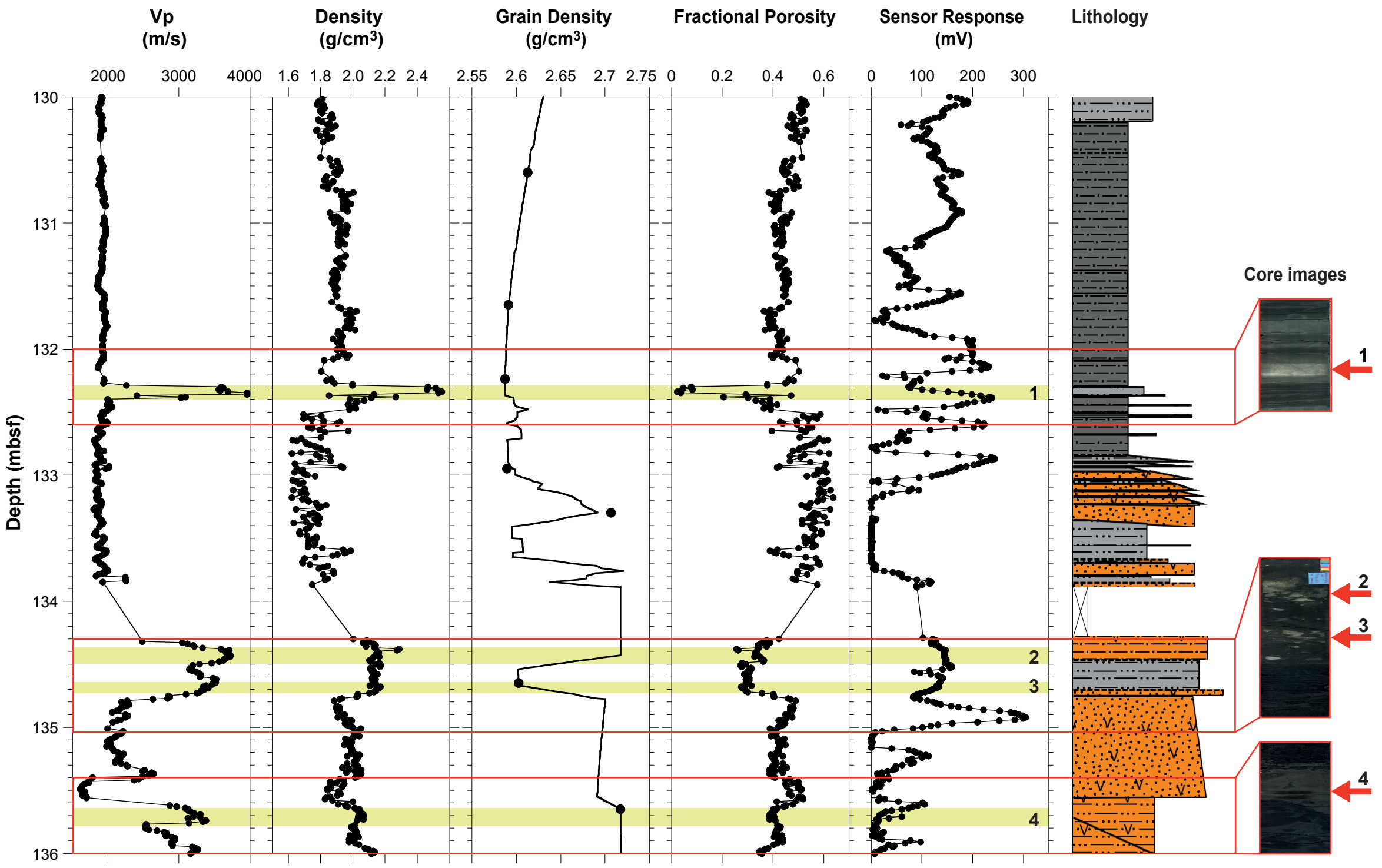
Vp
(m/s)
2000
3000
4000
Density
(g/cm3)
1.6
1.8
2.0
2.2
2.4
Grain Density
(g/cm3)
2.55
2.6
2.65
2.7
2.75
Fractional Porosity
0
0.2
0.4
0.6
Sensor Response
(mV)
0
100
200
300
Lithology
Depth (mbsf)
130
131
132
133
134
135
136
1
2
3
4
Core images
1
2
3
4

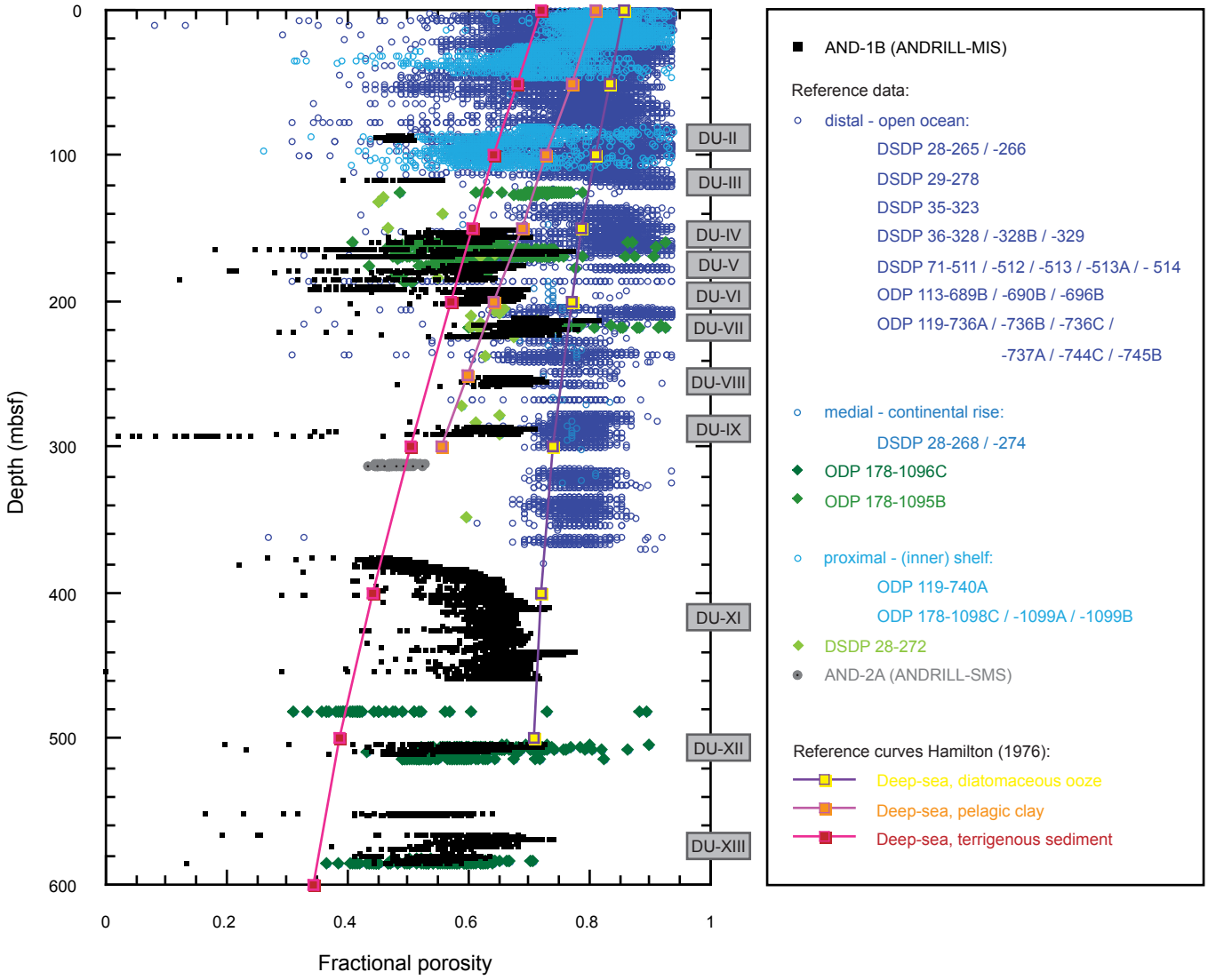
Depth (mbsf)
0
100
200
300
400
500
600
0
0.2
0.4
0.6
0.8
1
Fractional porosity
DU-II
DU-III
DU-IV
DU-V
DU-VI
DU-VII
DU-VIII
DU-IX
DU-XI
DU-XII
DU-XIII
AND-1B (ANDRILL-MIS)
Reference data:
distal - open ocean:
DSDP 28-265 / -266
DSDP 29-278
DSDP 35-323
DSDP 36-328 / -328B / -329
DSDP 71-511 / -512 / -513 / -513A / - 514
ODP 113-689B / -690B / -696B
ODP 119-736A / -736B / -736C /
-737A / -744C / -745B
medial - continental rise:
DSDP 28-268 / -274
ODP 178-1096C
ODP 178-1095B
proximal - (inner) shelf:
ODP 119-740A
ODP 178-1098C / -1099A / -1099B
DSDP 28-272
AND-2A (ANDRILL-SMS)
Reference curves Hamilton (1976):
Deep-sea, diatomaceous ooze
Deep-sea, pelagic clay
Deep-sea, terrigenous sediment